[CANCER RESEARCH 64, 3458–3464, May 15, 2004]

Genetic Analysis of Macrophage Characteristics as a Tool to Identify Tumor Susceptibility Genes: Mapping of Three Macrophage-Associated Risk Inflammatory Factors, *Marif1*, *Marif2*, and *Marif3*

Remond J. A. Fijneman,[1] Mariska Vos,[1] Johannes Berkhof,[2] Peter Demant,[3] and Georg Kraal[1]

[1]Department of Molecular Cell Biology and Immunology and [2]Department of Clinical Epidemiology and Biostatistics, VU University Medical Center, Amsterdam, the Netherlands, and [3]Department of Molecular and Cellular Biology, Roswell Park Cancer Institute, Buffalo, New York

ABSTRACT

Genetic predisposition to cancer is influenced by allelic variation in tumor susceptibility genes (TSGs) as present in the germline. We previously demonstrated in the mouse that TSGs frequently participate in genetic interactions, indicating that they represent molecular networks. Inflammation may constitute one of the molecular networks underlying susceptibility to cancer by influencing the tumor microenvironment. Because macrophages play a key role in inflammation and are often associated with tumors, we argue that a subset of TSGs can be identified by examining the genetics of macrophage characteristics. A panel of inflammation-related assays was established to phenotype mouse bone marrow-derived macrophages, which included stimulation with lipopolysaccharides followed by measurement of secretion of tumor necrosis factor α and the p40 chain of interleukin-12 and of expression of inducible nitric oxide synthase and cyclooxygenase-2. This panel of assays was used for linkage analysis and applied to bone marrow-derived macrophages derived from individual mice of segregating crosses between inbred strain O20 and the highly related strains NTX-10 and NTX-20, which differed from O20 in only 10% of their genome, to reduce genetic complexity. Three macrophage-associated risk inflammatory factors were mapped—*Marif1*, *Marif2*, and *Marif3*—that each affected several inflammation-related assays, confirming that they function within molecular networks. Moreover, *Marif1* and *Marif2* were localized in regions with established linkage for both quantitative and qualitative aspects of lung cancer susceptibility. These studies provide a novel approach to investigate the genetics of microenvironmental influence on predisposition to tumorigenesis, thereby contributing to development of new strategies that aim to prevent or treat cancer.

INTRODUCTION

Cancer is a complex disease that is influenced by both genetic and environmental factors. Identification of tumor susceptibility genes (TSGs) is crucial to identify the origin of variation in genetic predisposition to cancer and provides essential information to understand the molecular basis of tumor development. Several TSGs have been identified from families that exhibited Mendelian inheritance patterns of tumor incidence due to germline transmittance of one cancer-predisposing allele with very high penetrance toward the tumor phenotype (1). Although these high-penetrance TSGs have revolutionized clinical practice, their incidence among the human population is low, and collectively, familial forms of cancer account for less than 10% of all cancer cases (2, 3). Importantly, predisposition to the 90% of nonfamilial, sporadic forms of cancer is also strongly influenced by hereditary factors (4). However, identification of this group of TSGs from the human population is hampered by their low penetrance toward the cancer phenotype and their multiplicity. Reduction of genetic and environmental heterogeneity by using inbred strains of mice as a model for tumorigenesis in humans has proven to be an excellent tool to unravel the complexity of tumor susceptibility. By now, more than 100 TSGs have been mapped onto the mouse genome and several TSGs have been identified (5, 6). We previously mapped a total of 30 susceptibility to lung cancer loci, *Sluc1–Sluc30*, by making use of recombinant congenic strains, a system of mouse inbred strains specifically developed to dissect multigenic traits in which each recombinant congenic strain shares 12.5% of its genes from a common donor strain onto a background of 87.5% genes derived from a common background strain. Importantly, this reduction in genetic complexity allowed us to incorporate a systematic search for pair-wise epistatic interactions between TSGs, which revealed that 29 out of 30 *Sluc* loci were involved in one or more genetic interactions with other *Sluc* loci or sex of the mice (7–9). Similar results were obtained when this strategy was applied to studies of susceptibility to colon cancer (10–12). These studies clearly demonstrated that each TSG can have considerable main effects despite their multiplicity, however, these effects were masked by their participation in genetic interactions. The multitude of genetic interactions implies that they represent complex molecular networks underlying cancer predisposition.

Tumorigenesis is characterized by accumulation of genetic changes in the genome of cancer cells. Somatically acquired mutations in oncogenes and tumor suppressor genes result in dominant gain-of-function and recessive loss-of-function alterations, respectively, providing cancer cells with enhanced proliferation and survival rates compared with normal cells. Therefore, allelic variants of oncogenes and tumor suppressor genes form one group of candidate genes for TSGs. However, cancer cells *in vivo* are embedded within a microenvironment containing normal cells, and it has become increasingly clear that the interaction between transformed malignant cells and nontransformed cells like fibroblasts, endothelial cells, and immune cells is critical to cancer pathogenesis (13). The observation that many cancers arise from sites of infection, chronic irritation, and inflammation supports the notion that inflammatory cells contribute significantly to the neoplastic process (14, 15). Evidence that genetic variation in hematopoietic cells affects susceptibility to tumors of nonhematopoietic origin was provided by elegant experiments in which skin tumor initiation and progression was examined upon transplantation of bone marrow obtained from matrix metalloproteinase-9-proficient and -deficient mice (16). Moreover, aspirin and other nonsteroidal anti-inflammatory drugs reduce the number of intestinal tumors and lung tumors in mice (17, 18), whereas in humans, nonsteroidal anti-inflammatory drugs have been demonstrated to reduce the number of colorectal tumors (19, 20). These data illustrate that inflammation constitutes one of the molecular networks underlying susceptibility to cancer and indicate that genes expressed by hematopoietic cells to mediate inflammatory responses form another group of candidate genes for TSGs. Macrophages play a key role in both inflammation and tumorigenesis. Their phenotypic plasticity allows

Received 12/3/03; revised 2/26/04; accepted 3/3/04.

Grant support: Dutch Cancer Society Grant VU2000-2350.

The costs of publication of this article were defrayed in part by the payment of page charges. This article must therefore be hereby marked *advertisement* in accordance with 18 U.S.C. Section 1734 solely to indicate this fact.

Requests for reprints: Remond J. A. Fijneman, Department of Molecular Cell Biology and Immunology, VU University Medical Center, P.O. Box 7057, 1007 MB Amsterdam, the Netherlands. Phone: 31-20-4448079; Fax: 31-20-4448081; E-mail: RJA.Fijneman@vumc.nl.

them to initiate inflammatory responses by functioning as sensors for pathogens as well as to suppress inflammatory responses by functioning as professional phagocytes that efficiently remove apoptotic cells (21, 22). Moreover, macrophages are often present within the tumor microenvironment where they are both a source and a target of many cytokines, chemokines, and other signaling molecules, thereby contributing both positively and negatively to various stages of tumorigenesis by influencing processes like angiogenesis, tissue remodeling, and subversion of antitumor immunity (23).

We applied a novel strategy to identify a subset of TSGs that affect susceptibility to tumors of nonhematopoietic origin through their function in hematopoietic cells. Instead of investigating the heterogeneous process of tumorigenesis *in vivo*, we predicted that TSGs that influence susceptibility to cancer through their function in macrophages can be revealed by analysis of the genetics of inflammation-related macrophage characteristics *in vitro*. Primary bone marrow-derived macrophages (BMMf) were obtained from mice of segregating crosses between inbred strains that were known to differ from each other in several *Sluc* loci and exposed to a panel of inflammation-related assays. Here, we report the mapping of three macrophage-associated risk inflammatory factors, *Marif1*, *Marif2*, and *Marif3*.

MATERIALS AND METHODS

Mice, Crosses, and Genotyping. Mouse inbred strains O20/A, B10.O20/Dem, NTX-10/Dem, and NTX-20/Dem (henceforth referred to as O20, B10.O20, NTX-10, and NTX-20, respectively) were originally obtained from Dr. P. Demant and maintained at the VU University Medical Center animal facilities. All experiments were approved by the animal experimentation ethics committee, according to local and governmental regulations. B10.O20 is an *H2* congenic strain that carries the $H2^{pz}$ haplotype of strain O20 on the C57BL/10 background (N8). O20 and B10.O20 are the parental strains of the O20-congenic-B10.O20 (OcB) strains, a series of recombinant congenic strains that each carry 12.5% of the B10.O20 genome onto an O20 background (6, 24). NTX-10 and NTX-20 were derived from strain OcB-9 by backcrossing to O20. F_2 hybrid mice were obtained from crosses between the common background strain O20 and each of the strains NTX-10 and NTX-20 and used for experiments between 10 and 20 weeks of age. Mice were sacrificed by asphyxiation in CO_2, and DNA was isolated from their tails followed by genotyping with simple sequence length polymorphism markers according to standard procedures (7). Marker positions were derived from the mouse genome database (MGI 2.97).[4] All F_2 mice were typed for the markers *D2Mit156*, *D4Mit54*, *D4Mit126*, *D6Mit36*, *D8Mit155*, *D8Mit3*, *D8Mit125*, and *D19Mit60*. In addition, (O20 × NTX-10)F_2 mice were typed for *D4Mit12*, *D16Mit9*, *D19Mit61*, and *D19Mit3*, and (NTX-20 × O20)F_2 mice were typed for *D2Mit56*, *D6Mit52*, *D7Nds2*, and *D11Mit15*. On average, the B10.O20-derived genomic segments covered 145 cM of the NTX-10 genome distributed over six chromosomes and 131 cM of the NTX-20 genome distributed over seven chromosomes.

BMMf Cultures, Lipopolysaccharide (LPS) Treatment, and Detection of Tumor Necrosis Factor α (TNF-α), the p40 Chain of Interleukin-12 (IL-12p40), and Nitric Oxide (NO). Femurs and tibiae of adult mice were flushed with PBS. Bone marrow cells were plated in 145-mm bacteriological plastic Petri dishes (Greiner, Frickenhausen, Germany) and cultured in a 37°C incubator containing 5% CO_2. BMMf were obtained by differentiation of bone marrow cells in RPMI 1640 (Life Technologies, Paisley, United Kingdom) containing 10% heat-inactivated FCS (HyClone, Logan, UT), 100 units/ml penicillin, 100 μg/ml streptomycin, 2 mM L-glutamine (BioWhittaker, Verviers, Belgium), and 20 mM 4-(2-hydroxyethyl)-1-piperazineethanesulfonic acid (Life Technologies), supplemented with 15% (v/v) L929-conditioned medium as a source of colony-stimulating factor-1 (25). After 8 days of culture, individual mice yielded an average of about 40×10^6 mature macrophages, conforming to classification by Leenen *et al.* (26), based on flow cytometric analysis using a FACSscan (Becton Dickinson, San Jose, CA). Monoclonal Abs were used directed against the markers F4/80, Mac-1α (M1/70), and Mac-2 (M3/38), all acquired as supernatants from hybridomas cultured in our laboratory. At 8 days, BMMf were harvested using PBS-dissolved lidocaine (Sigma, St. Louis, MO) and distributed into 24-well tissue culture plates (Greiner) in 500-μl aliquots at a concentration of 1×10^6 cells/ml. BMMf were allowed to adhere and recover overnight, and then they were treated by replacement of the medium, now containing 0, 1, or 100 ng/ml LPS from *Escherichia coli* (0111:B4; Difco Laboratories, Detroit, MI). Supernatants were collected at various time points after treatment. Secretion of NO was estimated by measuring NO_2 levels using Griess reagent. Levels of TNF-α and IL-12 (the p40-chain) were determined by ELISA according to recommendations of the manufacturers (PharMingen, San Diego, CA, and Biosource, Fleurus, Belgium, respectively).

Immunofluorescent Staining and Quantification of Inducible NO Synthase (iNOS) and Cyclooxygenase-2 (COX-2) Expression. At 8 days of culture, BMMf were distributed into 24-well plates containing glass coverslips in aliquots of 500 μl at 2.5×10^5 cells/ml. BMMf were allowed to adhere and recover overnight before treatment with 0 or 100 ng/ml LPS for 24 h. Cells were washed in PBS supplemented with 0.1% (w/v) BSA (fraction V; Sigma), fixed in 2% paraformaldehyde in PBS for 10 min, permeabilized in methanol at −20°C for 20 min, and blocked in PBS supplemented with 0.1% (w/v) BSA containing 2.5% normal goat serum (Life Technologies). Cells were incubated with primary antibodies directed against iNOS (rabbit polyclonal) and COX-2 (mouse monoclonal) obtained from Transduction Laboratories (Lexington, KY) diluted in blocking solution for 1 h, followed by incubation with FITC-conjugated goat-antirabbit IgG (Jackson ImmunoResearch, West Grove, PA) and Alexa594-conjugated goat-antimouse IgG (Molecular Probes, Leiden, the Netherlands) secondary antibodies together with 0.5 μg/ml Hoechst dye 33258 (bisbenzimide; Sigma) to stain the nuclei. Samples were mounted in vinol mounting media (27), and results were viewed using a Nikon Eclipse E800 microscope equipped with epi-fluorescence optics and appropriate filters that allowed detection of FITC, Alexa594, and Hoechst dye. Filters were used to capture separate digital images for iNOS, COX-2, and nuclei from identical, randomly selected microscopical fields (×20 objective) using a DXM1200 Nikon digital camera. Each image was saved as a TIFF file with a resolution of 1280 × 1024 pixels. Staining for iNOS and COX-2 was quantified using Scion Image software (version β 4.0.2). Each image was converted to gray-scale and inverted, resulting in pixel values ranging from 0 to 255 that represented staining intensity. Areas that stained positive were automatically selected for measurements. Total staining intensity per selected area was calculated by multiplying the number of pixels/area with the area mean intensity. Addition of these values for all areas/microscopical field for iNOS (COX-2, respectively) divided by the number of nuclei present in the corresponding field revealed values representing relative mean iNOS (COX-2, respectively) protein levels per cell. More than 500 cells obtained from three separate microscopical fields were analyzed for each experimental condition.

Statistical Analysis. Cultures of BMMf were initiated in "experimental groups" of five F_2 mice at a time together with one age-matched female O20 mouse that was taken along as a common point of reference. All data were related to values acquired for the corresponding O20 reference mouse and ^{e}log-transformed to obtain approximately normal distributions. Statistical evaluation of each F_2 cross for linkage with inflammation-related assays was performed using ANOVA (GLM ANOVA; NCSS, Kaysville, UT). A full polygenic model was created that included main effects of one genetic marker per chromosomal segment and sex of the mice (fixed factors) together with "experimental group" (random factor). Markers were dropped sequentially by backward elimination using a 5% significance threshold per test until all remaining markers revealed nominal P values <0.05. Similar procedures were followed for statistical evaluation when the datasets of the (O20 × NTX-10)F_2 cross and the (NTX-20 × O20)F_2 cross were combined, in which case the full polygenic model included only those markers that were B10.O20-derived in both NTX-10 and NTX-20 while "experimental group" was used as a nested factor within "cross" (fixed factor). Genome-wide P values were calculated according to the rules of Lander and Kruglyak (28) in which the F-ratio from ANOVA was used for T^2 (11).

[4] http://www.informatics.jax.org/.

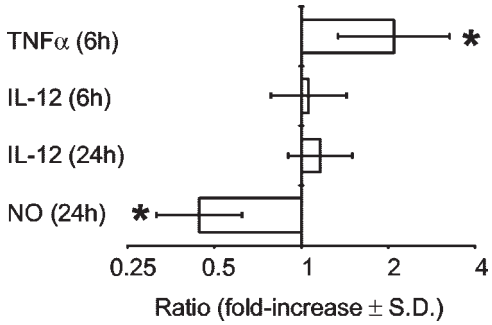

Fig. 1. Differential effects of stimulation of O20 BMMf with 1 ng/ml LPS compared with 100 ng/ml LPS on secretion of TNF-α, IL-12p40, and NO. The *horizontal axis* represents the ratio of secretion of TNF-α at 6 h (IL-12p40 at 6 h, IL-12p40 at 24 h, and NO at 24 h, respectively) after stimulation with 1 ng/ml LPS compared with 100 ng/ml LPS (mean values $\pm$ SD; $n = 10$). $*$, significant differences ($P < 0.001$; one-sample t test).

RESULTS

Establishing a Panel of Inflammation-Related Assays to Phenotype Macrophage Characteristics. BMMf were obtained by differentiation of bone marrow cells *in vitro* in the presence of colony-stimulating factor-1. This procedure yielded sufficient primary macrophages from individual mice to perform a series of inflammation-related assays. BMMf from strain O20 were used to select the optimal conditions to establish a panel of inflammation-related assays, because this strain was used as a common point of reference throughout these studies. Harvesting supernatants at 6 and 24 h after stimulation with 100 ng/ml LPS appeared to be most informative to determine secretion of TNF-α, IL-12p40, and NO. At 6 h, TNF-α levels were near maximal, IL-12p40 levels were about half-maximal, and NO levels were not detectable yet; whereas at 24 h, TNF-α levels had dropped, IL-12p40 levels were near maximal, and NO levels were high (data not shown). Stimulation of O20 BMMf with 1 ng/ml LPS resulted in 2-fold higher levels of TNF-α and 2-fold lower levels of NO than stimulation with 100 ng/ml LPS (Fig. 1), indicating that BMMf were differentially activated by low and high concentrations of LPS. Expression of iNOS and COX-2, the enzymes responsible for the increased production of NO and prostaglandins during inflammation, respectively (29, 30), was visualized by immunofluorescent staining. Hardly any staining was observed within 6 h after stimulation, confirming the absence of detectable levels of NO in supernatants at that point in time. Expression of both enzymes strongly increased at later time points, reaching near maximal levels at 24 h (Fig. 2). Their relative expression levels were estimated by computer-aided analysis of digital images.

The following experiments were selected to compose the panel of inflammation-related assays to be applied to linkage analysis studies: treatment of BMMf with 1 ng/ml and 100 ng/ml LPS followed by detection in supernatants of TNF-α at 6 h, IL-12p40 at 6 h and 24 h, and NO at 24 h after stimulation; and treatment of BMMf with 100 ng/ml LPS followed by determination of expression levels of iNOS and COX-2 at 24 h after stimulation. A pilot experiment was performed in which the characteristics for this panel of assays of O20 BMMf were compared with B10.O20 BMMf, the parental strains of the O20-congenic-B10.O20 (OcB) recombinant congenic strains that were previously used to map *Sluc* lung cancer susceptibility loci (31). About 1.5–2-fold differences were observed for all assays except for secretion of NO (data not shown), demonstrating that these assays were influenced by genetic variation between O20 and B10.O20. Although the magnitude of the differences appeared to be modest, it should be emphasized that large differences are not required to allow mapping of numerous susceptibility genes with relatively large effects, as demonstrated by the mapping studies of *Sluc* loci (7–9). Hence, this panel of inflammation-related assays was used for linkage analysis to phenotype macrophage characteristics.

Results of Linkage Analysis. Mapping genes involved in multigenic traits is greatly facilitated by reducing genetic complexity. Previously, we demonstrated that O20 and OcB-9 differ from each other in 11 *Sluc* loci, whereas genetically OcB-9 carries only 12.5% B10.O20-derived genome onto an O20 genetic background (7–9). Here, genetic complexity was even further reduced by making use of the OcB-9-derived strains NTX-10 and NTX-20, two strains that together differ from the common background strain O20 in only 10% of their genome that harbors seven *Sluc* loci. The B10.O20-derived genomic segments that were contained within NTX-10 and NTX-20 are listed in Table 1. First, BMMf were cultured from 30 (NTX-10 $\times$ O20)F_2 mice and exposed to the panel of inflammation-related assays. Genotypes of F_2 mice were determined using simple sequence length polymorphism markers located within each of the segregating genomic segments (Table 1; see "Materials and Methods"). One marker per segregating segment and sex of the mice were incorporated together in a statistical model to analyze their effects on each of the assays. Table 2 summarizes the results and presents both suggestive linkage data (nominal P values < 0.05) and genome-wide significant linkage data [P values < 0.05 after correction according to the

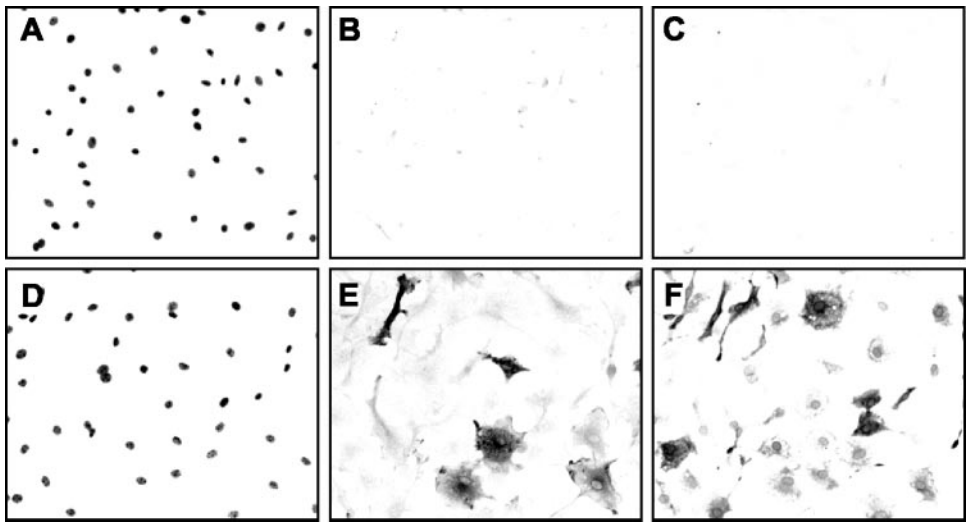

Fig. 2. Staining of O20 BMMf used to quantify expression of iNOS and COX-2. BMMf were stained by (immuno)fluorescence to visualize nuclei (*A* and *D*), expression of iNOS (*B* and *E*), and expression of COX-2 (*C* and *F*). Separate digital images were recorded from identical fields for each staining, representing unstimulated BMMf (*A–C*) and LPS-stimulated BMMf (100 ng/ml LPS for 24 h; *D–F*). Expression levels of iNOS and COX-2 were estimated by quantification of staining intensity using Scion Image software (version β 4.0.2).

Table 1 *Maximal and minimal B10.O20-derived genomic segments inherited by NTX-10 and NTX-20*

	NTX-10			NTX-20		
Chr[a]	Bordering markers and their position (cM)[b]	Maximal (cM)[c]	Minimal (cM)[d]	Bordering markers and their position (cM)[b]	Maximal (cM)[c]	Minimal (cM)[d]
2	D2Mit5 (5)-D2Mit56 (41)	36	22	D2Mit5 (5)-D2Mit35 (45)	40	31
4	D4Mit37 (57)-D4Mit42 (81)	24	14	D4Mit72 (60)-D4Mit42 (81)	21	5
6	D6Mit29 (37)-D6Mit10 (49)	12	7	D6Mit29 (37)-D6Mit10 (49)	12	7
6				D6Mit216 (59)-D6Mit13 (64)	5	2
7				D7Mit176 (27)-D7Mit98 (53)	26	15
8	acromere (0)-D8Mit129 (32)	32	23	acromere (0)-D8Mit129 (32)	32	23
11				D11Mit24 (28)-D11Nds1 (44)	16	7
16	acromere (0)-D16Mit101 (17)	17	8			
19	D19Mit32 (4)-telomere (53)	49	46	D19Mit61 (9)-D19Mit63 (24)	15	1

[a] The number of the chromosome (Chr) that contains a B10.O20-derived genomic segment.
[b] The SSLP markers that border the B10.O20-derived genomic segment and their position (in cM).
[c] The maximal length of the B10.O20-derived genomic segment (in cM).
[d] The minimal length of the B10.O20-derived genomic segment (in cM).

rules of Lander and Kruglyak (28)]. Significant linkage was obtained for sex of the mice with expression of iNOS; for D4Mit12 with secretion of TNF-α, with expression of iNOS, and with differential effects of low and high concentrations of LPS on secretion of IL-12p40; and for D8Mit3 with secretion of TNF-α. In addition, D19Mit60 was suggestively linked to expression of iNOS and to differential effects of low and high LPS concentrations on secretion of IL-12p40 (Table 2). These data indicated that loci on chromosomes 4, 8, and possibly 19 together with sex of the mice affected macrophage characteristics, as reflected by their influence on this panel of inflammation-related assays.

Strain NTX-20 contained B10.O20-derived genomic segments on chromosomes 4, 8, and 19 that largely overlapped the B10.O20-derived genomic regions in NTX-10 (Table 1). Although the marker D4Mit12 was not B10.O20-derived in NTX-20, several other nearby markers were, allowing improvement of the mapping position of the locus on chromosome 4. In addition, NTX-20 could be used to confirm a locus on chromosome 8 and to provide additional evidence for a locus on chromosome 19. Therefore, BMMf from 35 (NTX-20 $\times$ O20)F_2 mice were genotyped and phenotyped for the panel of inflammation-related assays. Statistical analysis revealed genome-wide significant linkage for D8Mit125 with secretion of TNF-α and suggestive linkage for D4Mit54 and sex of the mice with various assays (Table 2), confirming the presence of loci on chromosomes 4

Table 2 *Linkage data of the (NTX-10 $\times$ O20)F_2 and (O20 $\times$ NTX-20)F_2 crosses*

				Marif1	*Marif2*	*Marif3*
Assay (LPS in ng/ml; duration in hours)[a]	(NTX-10 $\times$ O20) or (O20 $\times$ NTX-20)[b]	*P* value (P) and corrected P (CP)[c]	Sex[d]	D4Mit12 or D4Mit54[e]	D8Mit3 or D8Mit125[f]	D19Mit60[g]
TNF-α (1; 6h)	NTX-10	P	0.0027	0.0053	0.000696	
		CP			**0.043**	
	NTX-20	P	0.028	0.012	0.00051	
		CP			**0.034**	
	NTX-10 and NTX-20	P	0.00078	0.00039	0.00046	
		CP		**0.021**	**0.0032**	
TNF-α (100; 6 h)	NTX-10	P	0.00086	0.00062	0.00029	
		CP		**0.039**	**0.021**	
	NTX-20	P	0.016		0.0065	
	NTX-10 and NTX-20	P	0.000002	0.00031	<0.000001	
		CP	**0.00031**	**0.017**	**<0.000001**	
IL-12 (1; 6 h)	NTX-10 and NTX-20	P			0.000003	0.00030
		CP			**0.00026**	**0.016**
IL-12 (100; 6 h)	NTX-10	P		0.0093		
	NTX-10 and NTX-20	P		0.000083	0.036	
		CP		**0.0052**		
IL-12 (100; 24 h)	NTX-10	P		0.011	0.0048	
	NTX-20	P	0.011	0.011		
	NTX-10 and NTX-20	P	0.00057	0.000017	0.040	0.0096
		CP	**0.040**	**0.0012**		
iNOS (100; 24 h)	NTX-10	P	0.00030	0.00072	0.0013	0.025
		CP	**0.030**	**0.042**		
	NTX-20	P	0.0057			
	NTX-10 and NTX-20	P	<0.000001	0.000027	<0.000001	0.020
		CP	**<0.000001**	**0.0019**	**0.000031**	
IL-12 (1 *versus* 100; 24 h)	NTX-10	P		0.00048		0.0045
		CP		**0.028**		
	NTX-10 and NTX-20	P		0.000013		0.000007
		CP		**0.00095**		**0.00054**

[a] This column lists the type of inflammation-related assay, the amount of LPS used to stimulate BMMf (1 ng/ml or 100 ng/ml), and the duration of stimulation before the assay was performed (in hours). Assays: tumor necrosis factor (TNF-α), secretion of TNF-α; IL-12, secretion of IL-12p40; iNOS, expression of iNOS; IL-12 (1 *versus* 100), differential effects of low and high concentrations of lipopolysaccharide (LPS) on secretion of IL-12p40.
[b] Data represent statistical evaluation of the (NTX-10 $\times$ O20)F_2 cross (NTX-10) the (O20 $\times$ NTX-20)F_2 cross (NTX-20); or the combination of both crosses (NTX-10 and NTX-20).
[c] Suggestive linkage represented by nominal *P* values $<$ 0.05 (P) and genome-wide significant linkage represented by corrected *P* values $<$ 0.05 (CP), according to the rules of Lander and Kruglyak (28).
[d] Effects of sex of the mice on inflammation-related assays. Data represent *P* values.
[e] Effects of *Marif1* on inflammation-related assays. *P* values listed for the (NTX-10 $\times$ O20)F_2 cross were obtained using the marker *D4Mit12*, whereas *P* values listed for the (O20 $\times$ NTX-20)F_2 cross and for the combination of both crosses were obtained using the marker *D4Mit54*.
[f] Effects of *Marif2* on inflammation-related assays. *P* values listed for the (NTX-10 $\times$ O20)F_2 cross were obtained using the marker *D8Mit3*, whereas *P* values listed for the (O20 $\times$ NTX-20)F_2 cross and for the combination of both crosses were obtained using the marker *D8Mit125*.
[g] Effects of *Marif3* on inflammation-related assays. All *P* values were obtained using the marker *D19Mit60*.

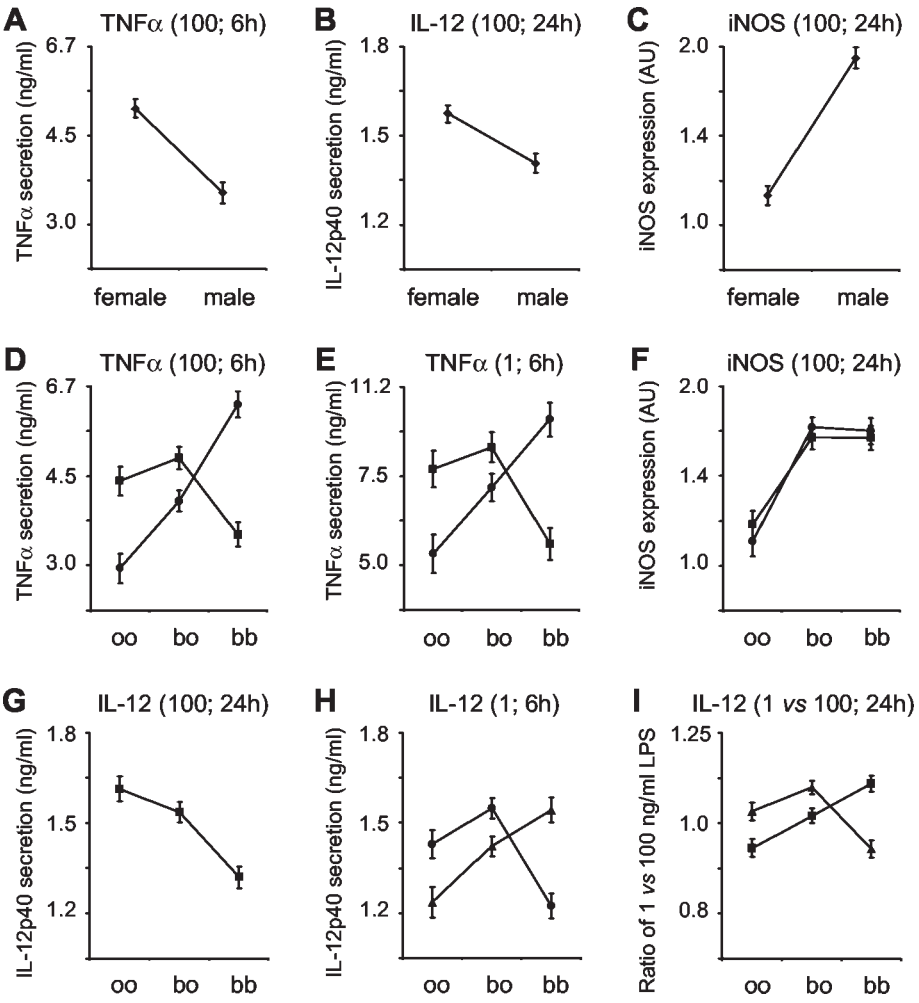

Fig. 3. Significant effects of sex and *Marif* loci on the panel of inflammation-related assays used to phenotype BMMf characteristics. Figures indicate magnitude and direction of the influence of sex of the mice (♦) and genotypes of *Marif1* (■), *Marif2* (●), and *Marif3* (▲), based on linkage analysis results when data from the (NTX-10 × O20)F_2-cross and (O20 × NTX-20)F_2-cross were combined (see Table 2 for *P* values). Concentrations of LPS and duration of stimulation are indicated between brackets in each figure (1 ng/ml or 100 ng/ml LPS; 6 h or 24 h). Sex of the mice influenced secretion of TNF-α (*A*), secretion of IL-12p40 (*B*), and expression of iNOS (*C*). *Marif1* and *Marif2* affected secretion of TNF-α (*D* and *E*) and expression of iNOS (*F*). *Marif1* also affected secretion of IL-12p40 upon stimulation of BMMf with 100 ng/ml LPS for 24 h (*G*), whereas *Marif2* and *Marif3* affected IL-12p40 secretion upon stimulation with 1 ng/ml LPS for 6 h (*H*). In addition, *Marif1* and *Marif3* affected secretion of IL-12p40 in an LPS-concentration-dependent manner, indicated by the ratio of stimulation of BMMf with 1 ng/ml LPS *versus* stimulation with 100 ng/ml LPS (1 *versus* 100) for 24 h (*I*). Data represent mean values ± SE on ^{e}log-scaled *Y* axes; *AU*, arbitrary units; *oo*, homozygosity for the O20 allele; *bo*, heterozygosity; and *bb*, homozygosity for the B10.O20 allele.

and 8. Next, the datasets from the (O20 × NTX-10)F_2 and (NTX-20 × O20)F_2 crosses were combined for statistical evaluation to improve linkage results for loci on chromosomes 4 and 8 and to allow detection of a putative locus on chromosome 19. This procedure revealed genome-wide significant linkage between TNF-α secretion and sex, D4Mit54, and D8Mit125; between IL-12p40 secretion and sex, D4Mit54, D8Mit125, and D19Mit60; between iNOS expression and sex, D4Mit54, and D8Mit125; and between differential effects of low and high concentrations of LPS on IL-12p40 secretion and D4Mit54 and D19Mit60 (Table 2). No significant linkage was found with secretion of NO or expression of COX-2. These data demonstrate that various macrophage inflammation-related characteristics are affected by sex of the mice and loci on chromosomes 4, 8, and 19, which we named macrophage-associated risk inflammatory factors *Marif1*, *Marif2*, and *Marif3*, respectively. The magnitude and direction of effects of sex of the mice, *Marif1*, *Marif2*, and *Marif3* are indicated in Fig. 3. The chromosomal positions of *Marif* loci onto the mouse genome are presented in Fig. 4.

DISCUSSION

Dissecting the genetics of susceptibility to cancer is hampered by its multigenic nature and complex phenotype. Previously, we demonstrated that susceptibility to cancer is influenced by many TSGs that are frequently involved in genetic interactions, which illustrated the extensive complexity of genetic predisposition to cancer and emphasized the necessity to reduce this to identify new TSGs (7–9). Here, we applied a novel strategy in which reduction of genetic complexity was combined with reduction of phenotypic complexity. Genetic complexity was reduced by making use of highly related inbred strains of mice, strains that differed from each other in only 10% of their genome. Phenotypic complexity was reduced by selecting one of the biological processes known to contribute to tumorigenesis for analysis *in vitro*, instead of studying the complex multicellular and multistep development of cancer *in vivo*. The intimate relation between cancer and inflammation combined with the fact that macrophages are capable to mediate both tumorigenesis and inflammatory responses lead to the prediction that a subset of TSGs affect predisposition to cancer through their influence on macrophage characteristics. Using segregating crosses between strains that were known to differ in several lung tumor susceptibility loci, we report here the mapping of three macrophage-associated risk inflammatory factors, *Marif1*, *Marif2*, and *Marif3*. These studies highlight several important features of complex multigenic traits. First, only 10% of the genome was analyzed for linkage (Table 1), yet three *Marif* loci were mapped, demonstrating once more that multigenic traits are truly influenced by many genes. Second, each *Marif* locus was linked to multiple inflammation-related assays (Table 2), supporting the notion that *Marif* genes function within molecular networks. As a consequence, each locus is expected to affect many assays, suggesting that even the restricted panel of inflammation-related assays that was applied here to determine macrophage characteristics might actually suffice to detect the majority of *Marif* loci. And third, the observation that allelic

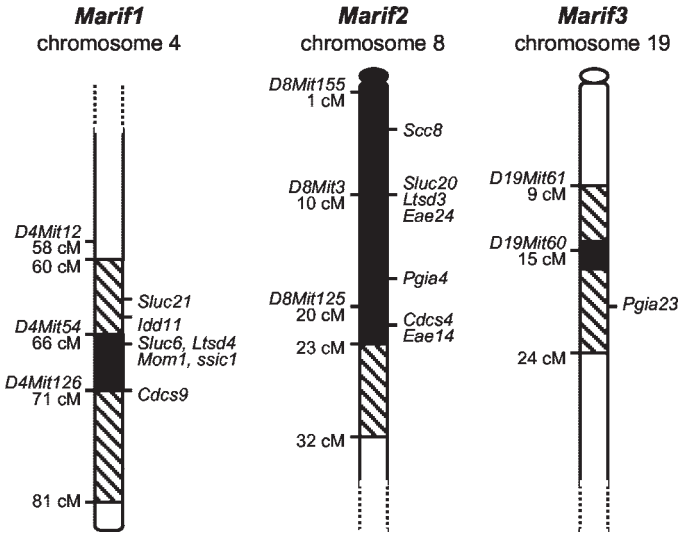

Fig. 4. Chromosomal positions of *Marif1*, *Marif2*, and *Marif3* loci onto the mouse genome. Schematic illustration of part of chromosomes 4, 8, and 19, in which *black areas* together with *hatched areas* represent the maximal size, and *black areas* alone represent the minimal size of B10.O20-derived genomic segments that contain a *Marif* locus, based on the B10.O20-derived regions that are commonly shared by NTX-10 and NTX-20 (Table 1). Markers used for genotyping and their positions (MGI 2.97)[4] are indicated on the left of each chromosome, whereas QTLs that were mapped to these regions are indicated on the right: *Sluc*, susceptibility to lung cancer (8, 9); *Ltsd*, lung tumor shape-determining (40); *ssic*, susceptibility to small intestinal cancer (42); *Mom1*, modifier of Apc^{Min}-induced intestinal neoplasia (41); *Scc*, susceptibility to colon cancer (11); *Cdcs*, cytokine deficiency-induced colitis susceptibility (43, 44); *Idd*, insulin-dependent diabetes susceptibility (45); *Eae*, experimental autoimmune encephalomyelitis susceptibility (46, 47); and *Pgia*, proteoglycan-induced arthritis (48, 49).

variation of *Marif* loci can have opposite effects on one assay, for instance illustrated by the effects of *Marif1* and *Marif2* on secretion of TNF-α (Fig. 3, *D* and *E*), confirmed that phenotypic variation between parental strains will often represent an underestimation of the total amount of variation that can be detected by linkage analysis.

The *Marif1* and *Marif2* loci were each shown to modulate secretion of TNF-α, secretion of IL-12p40, and expression of iNOS (Table 2). However, the opposite direction of their effects on secretion of TNF-α (Fig. 3, *D* and *E*) was contrasted by the similar direction of their effects on expression of iNOS (Fig. 3*F*), whereas they required different concentrations of LPS to affect secretion of IL-12p40 (Fig. 3, *G* and *H*). Moreover, allelic variation in *Marif3* resulted in opposite effects on secretion of IL-12p40 compared with *Marif2* (Fig. 3*H*) and in opposite effects on the ratio of low *versus* high concentrations of LPS on secretion of IL-12p40 compared with *Marif1* (Fig. 3*I*). Together, these data indicate that each locus influenced the molecular network of inflammation via different pathways, suggesting that their identification will help to unravel the mechanisms that determine macrophage versatility. Besides the inflammation-related assays that were linked to *Marif* loci, several assays from the panel revealed no linkage at all. For instance, no linkage was found with expression of COX-2 despite the observation that this assay was influenced by genetic variation between the parental strains O20 and B10.O20. Most likely, genes that modify COX-2 expression are present within the 90% of the genome that was not covered by the crosses used in this study. Alternatively, loci whose main effects are masked by genetic interactions could not be detected by our analysis because the number of mice involved in the (O20 $\times$ NTX-10)F_2 and (NTX-20 $\times$ O20)F_2 crosses was not large enough to allow a systematic search for epistatis. Absence of linkage with secretion of NO was an unexpected finding considering the fact that both *Marif1* and *Marif2* were linked to expression of iNOS, the enzyme responsible for the strong induction of NO production during an inflammatory response. However, also the O20 and B10.O20 parental strains exhibited this discrepancy because they differed in their expression of iNOS while producing similar amounts of NO (data not shown), indicating that iNOS is not the only factor that regulates the amount of NO production and secretion.

Tumorigenesis is a process in which both the acquisition of genetic alterations within cancer cells as well as the interaction between cancer cells and their microenvironment play a prominent role. Therefore, one group of candidate genes for TSGs include oncogenes and tumor suppressor genes, exemplified by identification of *Kras2* as a susceptibility gene for lung cancer and *Ptprj* as a susceptibility gene for colon cancer (32, 33). Another group of candidate genes for TSGs comprises genes that influence the (tumor) microenvironment, exemplified by identification of the group IIA secretory phospholipase A_2 gene *Pla2g2a* as a susceptibility gene for Apc^{Min}-induced intestinal neoplasia (34, 35). Our strategy specifically aimed to map TSGs that affect susceptibility to cancer through their influence on the (tumor) microenvironment and resulted in the mapping of *Marif* loci that influence the characteristics of macrophages, one of the nontransformed nonepithelial cell types that is frequently associated with tumors of epithelial origin. Although these data do not prove that *Marif* genes are TSGs, they each do affect parameters that have been implicated to affect tumorigenesis: mice deficient for TNF-α become more resistant to skin carcinogenesis (36), whereas mice that lack iNOS are more susceptible to intestinal cancer and less susceptible to lung cancer (37, 38). The adaptive immune response is strongly influenced by IL-12, and absence of IL-12p40 from antigen-presenting cells results in poor cytotoxic T lymphocyte responses against tumors (39). Because of the multitude of effects that macrophages have on the tumor microenvironment, *Marif* loci that affect tumor susceptibility through their function in macrophages are likely to influence both quantitative and qualitative features of various types of cancer (23). In addition, *Marif* loci are also expected to affect susceptibility to other diseases in whose etiology macrophages play an important role, like inflammatory diseases and autoimmune diseases. In compliance with these expectations, *Marif1* and *Marif2* colocalized with quantitative trait loci (QTLs) for susceptibility to lung cancer, *Sluc6/Sluc21* and *Sluc20*, respectively (8, 9); with QTLs that determine lung tumor shape, *Ltsd4* and *Ltsd3*, respectively (40); with susceptibility to intestinal cancer, *Mom1/ssic1* and *Scc8*, respectively (11, 41, 42); with susceptibility to colitis, *Cdcs9* and *Cdcs4*, respectively (43, 44); and with susceptibility to autoimmune diseases like diabetes and experimental allergic encephalomyelitis, *Idd11* and *Eae14*/*Eae24*, respectively (Refs. 45–47; Fig. 4). Moreover, *Marif2* and *Marif3* colocalized with QTLs for susceptibility to arthritis, *Pgia4* and *Pgia23*, respectively (48, 49). This clustering of QTLs for susceptibility to various macrophage-associated diseases suggests that they could be influenced by one gene that affects macrophage characteristics, represented by the *Marif* locus. At present, the genomic segments to which the *Marif* loci have been mapped are relatively large, and each region contains several hundreds of genes, including many putative candidate genes that are involved in inflammation. It is interesting to note that *Marif1* is tightly linked to the secretory phospholipase A_2 gene *Pla2g2a*, which besides its effects on inflammation and predisposition to intestinal cancer was recently also shown to affect susceptibility to atherosclerosis when transgenically expressed by macrophages (50).

Additional investigations are required to identify the genes that affect macrophage characteristics *in vitro* followed by examination of their effects *in vivo* on quantitative and qualitative aspects of tumor development. These studies will extend our knowledge about the molecular mechanisms via which hematopoietic cells in general and macrophages in particular influence tumorigenesis, thereby increasing

our understanding of genetic predisposition to cancer and contributing to early diagnosis and prevention of cancer. Moreover, the possibility to manipulate nontumorigenic hematopoietic cells *ex vivo* to modulate tumorigenesis *in vivo* may provide additional tools to improve cancer treatment further.

ACKNOWLEDGMENTS

We thank E. van Gelderop and B. Jongmans for expert technical assistance and Dr. G. Bouma for helpful discussions and critical evaluation of the manuscript.

REFERENCES

1. Emery J, Lucassen A, Murphy M. Common hereditary cancers and implications for primary care. Lancet 2001;358:56–63.
2. Balmain A, Gray J, Ponder B. The genetics and genomics of cancer. Nat Genet 2003;33(Suppl):238–44.
3. Ponder BA. Cancer genetics. Nature 2001;411:336–41.
4. Pharoah PD, Antoniou A, Bobrow M, Zimmern RL, Easton DF, Ponder BA. Polygenic susceptibility to breast cancer and implications for prevention. Nat Genet 2002;31:33–6.
5. Balmain A. Cancer as a complex genetic trait: tumor susceptibility in humans and mouse models. Cell 2002;108:145–52.
6. Demant P. Cancer susceptibility in the mouse: genetics, biology and implications for human cancer. Nat Rev Genet 2003;4:721–34.
7. Fijneman RJ, de Vries SS, Jansen RC, Demant P. Complex interactions of new quantitative trait loci, Sluc1, Sluc2, Sluc3, and Sluc4, that influence the susceptibility to lung cancer in the mouse. Nat Genet 1996;14:465–7.
8. Fijneman RJ, Jansen RC, van der Valk MA, Demant P. High frequency of interactions between lung cancer susceptibility genes in the mouse: mapping of Sluc5 to Sluc14. Cancer Res 1998;58:4794–8.
9. Tripodis N, Hart AA, Fijneman RJ, Demant P. Complexity of lung cancer modifiers: mapping of thirty genes and twenty-five interactions in half of the mouse genome. J Natl Cancer Inst (Bethesda) 2001;93:1484–91.
10. van Wezel T, Stassen AP, Moen CJ, Hart AA, van der Valk MA, Demant P. Gene interaction and single gene effects in colon tumour susceptibility in mice. Nat Genet 1996;14:468–70.
11. van Wezel T, Ruivenkamp CA, Stassen AP, Moen CJ, Demant P. Four new colon cancer susceptibility loci, Scc6 to Scc9 in the mouse. Cancer Res 1999;59:4216–8.
12. Ruivenkamp CA, Csikos T, Klous AM, van Wezel T, Demant P. Five new mouse susceptibility to colon cancer loci, Scc11-Scc15. Oncogene 2003;22:7258–60.
13. Hanahan D, Weinberg RA. The hallmarks of cancer. Cell 2000;100:57–70.
14. Balkwill F, Mantovani A. Inflammation and cancer: back to Virchow? Lancet 2001;357:539–45.
15. Coussens LM, Werb Z. Inflammation and cancer. Nature 2002;420:860–7.
16. Coussens LM, Tinkle CL, Hanahan D, Werb Z. MMP-9 supplied by bone marrow-derived cells contributes to skin carcinogenesis. Cell 2000;103:481–90.
17. Jacoby RF, Marshall DJ, Newton MA, et al. Chemoprevention of spontaneous intestinal adenomas in the Apc Min mouse model by the nonsteroidal anti-inflammatory drug piroxicam. Cancer Res 1996;56:710–4.
18. Jalbert G, Castonguay A. Effects of NSAIDs on NNK-induced pulmonary and gastric tumorigenesis in A/J mice. Cancer Lett 1992;66:21–8.
19. Sandler RS, Halabi S, Baron JA, et al. A randomized trial of aspirin to prevent colorectal adenomas in patients with previous colorectal cancer. N Engl J Med 2003;348:883–90.
20. Baron JA, Cole BF, Sandler RS, et al. A randomized trial of aspirin to prevent colorectal adenomas. N Engl J Med 2003;348:891–9.
21. Gordon S. Alternative activation of macrophages. Nat Rev Immunol 2003;3:23–35.
22. Savill J, Dransfield I, Gregory C, Haslett C. A blast from the past: clearance of apoptotic cells regulates immune responses. Nat Rev Immunol 2002;2:965–75.
23. Mantovani A, Sozzani S, Locati M, Allavena P, Sica A. Macrophage polarization: tumor-associated macrophages as a paradigm for polarized M2 mononuclear phagocytes. Trends Immunol 2002;23:549–55.
24. Stassen AP, Groot PC, Eppig JT, Demant P. Genetic composition of the recombinant congenic strains. Mamm Genome 1996;7:55–8.
25. Hume DA, Gordon S. Optimal conditions for proliferation of bone marrow-derived mouse macrophages in culture: the roles of CSF-1, serum, Ca^{2+}, and adherence. J Cell Physiol 1983;117:189–94.
26. Leenen PJ, de Bruijn MF, Voerman JS, Campbell PA, van Ewijk W. Markers of mouse macrophage development detected by monoclonal antibodies. J Immunol Methods 1994;174:5–19.
27. Fukui Y, Yumura S, Yumura TK. Agar-overlay immunofluorescence: high-resolution studies of cytoskeletal components and their changes during chemotaxis. Methods Cell Biol 1987;28:347–56.
28. Lander E, Kruglyak L. Genetic dissection of complex traits: guidelines for interpreting and reporting linkage results. Nat Genet 1995;11:241–7.
29. Bogdan C. Nitric oxide and the immune response. Nat Immunol 2001;2:907–16.
30. Williams CS, Mann M, DuBois RN. The role of cyclooxygenases in inflammation, cancer, and development. Oncogene 1999;18:7908–16.
31. Fijneman RJ, van der Valk MA, Demant P. Genetics of quantitative and qualitative aspects of lung tumorigenesis in the mouse: multiple interacting susceptibility to lung cancer (Sluc) genes with large effects. Exp Lung Res 1998;24:419–36.
32. You M, Wang Y, Stoner G, et al. Parental bias of Ki-ras oncogenes detected in lung tumors from mouse hybrids. Proc Natl Acad Sci USA 1992;89:5804–8.
33. Ruivenkamp CA, van Wezel T, Zanon C, et al. Ptprj is a candidate for the mouse colon-cancer susceptibility locus Scc1 and is frequently deleted in human cancers. Nat Genet 2002;31:295–300.
34. MacPhee M, Chepenik KP, Liddell RA, Nelson KK, Siracusa LD, Buchberg AM. The secretory phospholipase A2 gene is a candidate for the Mom1 locus, a major modifier of ApcMin-induced intestinal neoplasia. Cell 1995;81:957–66.
35. Cormier RT, Hong KH, Halberg RB, et al. Secretory phospholipase Pla2g2a confers resistance to intestinal tumorigenesis. Nat Genet 1997;17:88–91.
36. Moore RJ, Owens DM, Stamp G, et al. Mice deficient in tumor necrosis factor-α are resistant to skin carcinogenesis. Nat Med 1999;5:828–31.
37. Scott DJ, Hull MA, Cartwright EJ, et al. Lack of inducible nitric oxide synthase promotes intestinal tumorigenesis in the Apc(Min/+) mouse. Gastroenterology 2001;121:889–99.
38. Kisley LR, Barrett BS, Bauer AK, et al. Genetic ablation of inducible nitric oxide synthase decreases mouse lung tumorigenesis. Cancer Res 2002;62:6850–6.
39. Camporeale A, Boni A, Iezzi G, et al. Critical impact of the kinetics of dendritic cells activation on the in vivo induction of tumor-specific T lymphocytes. Cancer Res 2003;63:3688–94.
40. Tripodis N, Demant P. Genetic analysis of three-dimensional shape of mouse lung tumors reveals eight lung tumor shape-determining (Ltsd) loci that are associated with tumor heterogeneity and symmetry. Cancer Res 2003;63:125–31.
41. Dietrich WF, Lander ES, Smith JS, et al. Genetic identification of Mom-1, a major modifier locus affecting Min-induced intestinal neoplasia in the mouse. Cell 1993;75:631–9.
42. Fijneman RJ, Demant P. A gene for susceptibility to small intestinal cancer, ssic1, maps to the distal part of mouse chromosome 4. Cancer Res 1995;55:3179–82.
43. Mahler M, Most C, Schmidtke S, et al. Genetics of colitis susceptibility in IL-10-deficient mice: backcross versus F2 results contrasted by principal component analysis. Genomics 2002;80:274–82.
44. Farmer MA, Sundberg JP, Bristol IJ, et al. A major quantitative trait locus on chromosome 3 controls colitis severity in IL-10-deficient mice. Proc Natl Acad Sci USA 2001;98:13820–5.
45. Morahan G, McClive P, Huang D, Little P, Baxter A. Genetic and physiological association of diabetes susceptibility with raised Na^+/H^+ exchange activity. Proc Natl Acad Sci USA 1994;91:5898–902.
46. Blankenhorn EP, Butterfield RJ, Rigby R, et al. Genetic analysis of the influence of pertussis toxin on experimental allergic encephalomyelitis susceptibility: an environmental agent can override genetic checkpoints. J Immunol 2000;164:3420–5.
47. Encinas JA, Lees MB, Sobel RA, et al. Identification of genetic loci associated with paralysis, inflammation and weight loss in mouse experimental autoimmune encephalomyelitis. Int Immunol 2001;13:257–64.
48. Otto JM, Cs-Szabo G, Gallagher J, et al. Identification of multiple loci linked to inflammation and autoantibody production by a genome scan of a murine model of rheumatoid arthritis. Arthritis Rheum 1999;42:2524–31.
49. Adarichev VA, Valdez JC, Bardos T, Finnegan A, Mikecz K, Glant TT. Combined autoimmune models of arthritis reveal shared and independent qualitative (binary) and quantitative trait loci. J Immunol 2003;170:2283–92.
50. Webb NR, Bostrom MA, Szilvassy SJ, Van Der Westhuyzen DR, Daugherty A, De Beer FC. Macrophage-expressed group IIA secretory phospholipase A2 increases atherosclerotic lesion formation in LDL receptor-deficient mice. Arterioscler Thromb Vasc Biol 2003;23:263–8.

Genetic Analysis of Macrophage Characteristics as a Tool to Identify Tumor Susceptibility Genes: Mapping of Three Macrophage-Associated Risk Inflammatory Factors, Marif1, Marif2, and Marif3

Remond J. A. Fijneman, Mariska Vos, Johannes Berkhof, et al.

Cancer Res 2004;64:3458-3464.